Journal of Advanced Marine Engineering and Technology, Vol. 50, No. 1, pp. 16~23, 2026
J. Advanced Marine Engineering and Technology (JAMET)
https://doi.org/10.5916/jamet.2026.50.1.16

ISSN 2234-7925 (Print)
ISSN 2765-4796 (Online)
Original Paper

Influence of injection timing and ammonia energy fraction on combustion and emission characteristics in a dual direct injection CI engine

Ardhika Setiawan[1] · Ocktaeck Lim[†]

(Received November 14, 2025 ; Revised December 21, 2025 ; Accepted February 6, 2026)

Abstract: The impact of ammonia and diesel ratios on combustion and emission properties of ammonia in AMMONIA direct injection (AMMONIA-Di) engines was examined through experimental and numerical studies. An adapted rapid compression expansion machine (RCEM) was employed to enable the dual fuel injection (diesel-ammonia) - compression ignition (CI) technique for the experiment. The experiment utilized a compression ratio (CR) of 19 and an ammonia energy percentage between 10% and 90%. Modifications were implemented to the start of injection (SOI) from 0 degrees to 40 degrees before top dead center (BTDC) to ascertain the optimal auto-ignition characteristics of ammonia. To promote auto-ignition, the diesel's start of injection (SOI) was set at 10 degrees before top dead center (BTDC). Computational fluid dynamics (CFD) modeling was employed to delineate the intricate emission dispersion during the combustion process. In the expansion phase, ammonia undergoes a secondary combustion stage, it shows that the fuel cannot completely combust during the first auto-ignition process. Emissions of CO2, HC, and NOx increase when direct injection compression ignition engines utilize up to 50% ammonia. When SOI is implemented for ammonia at 0 and 40 BTDC with an ammonia energy percentage over 50%, the emissions fluctuate considerably, signifying suboptimal combustion quality that promotes emission generation.

Keywords: Dual fuel engine, Ammonia engine, CFD modelling, Combustion and emission

1. Introduction

Several studies have shown that ammonia cars pollute far less than conventional fuel-powered vehicles **[1]**. Snelgrove et al. indicated that during emission by the European standard test at 25°C, an ammonia-fueled vehicle demonstrated a 40% reduction in hydrocarbons (HC), 60% reduction of carbon monoxide (CO), and significantly diminished CO2 emissions [2]. Moreover, ammonia produces very little NOx and almost no particulate matter since it contains less carbon than gasoline [3]. Moreover, ammonia produces very little NOx and almost no particulate matter since it contains less carbon than gasoline. Because ammonia has no carbon and burns stoichiometrically, its basic chemical structure reduces particulate matter emissions **[4]**. Diesel in a CI engine and ammonia-DI in a SI engine were contrasted by Sungha Baek et al. According to their findings, diesel fuel combustion results in the emission of 3.6 times the quantity of CO2-equivalent N2O and CH4 as compared to ammonia combustion **[5]**. Instead of using diesel on a SI engine, Windarto *et al.* employed 100% ammonia DI. He found during his investigation that diesel created more HC, CO, CO_2, and NOx than ammonia. But compared to ammonia, diesel has a thermal efficiency that is 14.26% higher. The ammonia fuel produced somewhat higher brake fuel consumption and improved engine thermal efficiency with longer spark duration **[6]**. The effect of ammonia-DI on SI engines has been the subject of numerous investigations. However, research on ammonia-DI in CI engines has been rather limited.

One of the most recent technological advancements is the dual-fuel combustion process, which uses two separate fuels, often natural gas and diesel, as the name suggests. Dual-fuel engines present several advantages relative to conventional diesel engines and those employing dual direct injection and ignition **[7]**. Natural gas has an interesting power-to-pollution ratio because of its low pollution rate and diesel's capacity to auto-ignite. Numerous studies on dual-fuel engine modeling, building, and design have been published **[8]**. Dual-fuel technology, either in its whole or as an add-on feature, has

† Corresponding Author (ORCID: https://orcid.org/0000-0001-8130-0838): Professor, Division of Mechanical and Automotive Engineering, University of Ulsan, 93 Daehak-ro, Nam-gu, Ulsan, 44610, South Korea, E-mail: otlim@ulsan.ac.kr, Tel: +82-52-259-2852

1 Researcher, Department of Mechanical and Automotive Engineering, University of Ulsan, E-mail: ardhika.s@gmail.com

been utilized by several engine manufacturers to create a variety of devices (automobiles, power plants). The intake temperature will be significantly lowered by using the ammonia injection method in the intake manifold. Consequently, diesel's auto-ignition properties deteriorate and volumetric efficiency is decreased. Large ammonia substitution ratios cannot be achieved via the intake manifold method due to its high percentage octane number in ammonia **[9]**. Determining the ideal injection timing position based on the properties of the fuel is crucial. An extended ignition delay brought on by early direct injection produces a better air-fuel combination prior to auto ignition. Nevertheless, in the context of liquid phase ammonia, early injection significantly lowers the temperature and disrupts diesel ignition. As a result, it is critical to explore the optimal start of injection for the direct injection of ammonia.

The ammonia dual direct injection (ammonia-diesel) fuel strategy with the ammonia-diesel ratio adjustment and the ammonia injection start (SOI) was experimentally and numerically studied in this work. Exhaust emissions, including CO_2, CO, HC, and NOx, thoroughly examined and discussed in connection with engine operation parameter.

2. Methodology

The RCEM is driven by an electric motor nominally operating at 1200 rpm. To ensure sufficient starting and transient torque during the compression stroke, a reduction gearbox is employed to decrease the crankshaft rotational speed to 240 rpm while proportionally amplifying the available torque. This configuration is necessary because the RCEM must accelerate the crankshaft and piston assembly from rest (0 rpm) to the target rotational speed within a single compression–expansion event, which requires substantially higher torque than steady-state engine operation.

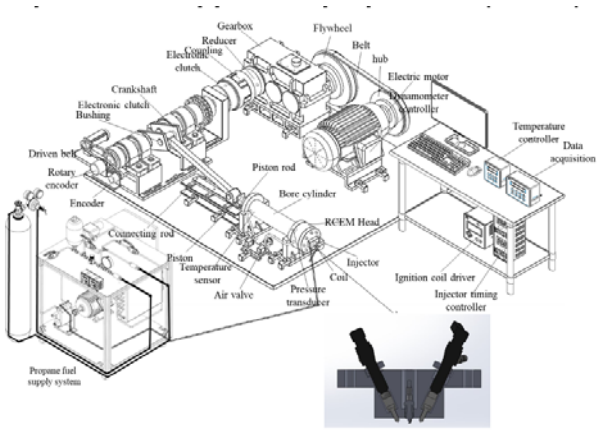

Figure 1: Rapid compression expansion machine

Table 1: Engine specification

Parameter	Specification
Cylinder bore and stroke	100 mm × 450 mm configuration
CR range	Adjustable from 10:1 up to 27:1
Ammonia injector type	Denso model 02210
Electric motor speed (drive)	1200 RPM
Crankshaft speed (after gearbox)	240RPM
Gear reduction ratio	5:1
Controlled temperature window	325 K to 415 K
Diesel injector model	Bosch 0445110327 (A-series)
Number of nozzle orifices	Seven holes
Injector Ammonia	Denso 02210

Note: The electric motor speed refers to the drive unit, while the crankshaft speed represents the mechanical output of the RCEM after gear reduction and is used as the reference speed for all combustion analyses.

Table 2: Fuel specification **[10]**

Property	Fuels	
	Diesel	NH3
Ignition quality (cetane rating)	44.9	—
Lower heating value (MJ per kg)	43.5	18.5
Density (kg/m³)	824	690 (liquid NH_3 at 300 K, 200 bar)
Auto-ignition threshold (°C)	227	652
Hydrogen-to-carbon ratio	1.77	—
Stoichiometric air–fuel requirement	14.4	6.05
Energy content per unit mass (kJ/kg)	269	—

Note: Density value corresponds to subcooled liquid ammonia at the injector inlet conditions used in this study. Temperature- and pressure-dependent phase change is accounted for through the spray evaporation model during injection.

Each test point was repeated three times to assess reproducibility, and the cycle-to-cycle variation of peak in-cylinder pressure remained within ±3%. This RCEM-based approach enables controlled, engine-representative single-cycle combustion analysis while avoiding cyclic variability associated with intake and exhaust processes. Such decoupling of mechanical drive constraints from thermodynamic equivalence is a well-established practice in RCEM and RCM-based combustion studies.

Ammonia (99.99% pure) and regular diesel were the main fuels used in this experiment. In Korea, it was acquired from a local gas station. To identify the energy content of diesel and ammonia, the fuel is labeled "AEF 10 to AEF 90"; the final digit indicates the percentage of diesel energy, while "AEF" denotes ammonia energy fraction. A Bosch injector and a Denso fuel injection mass flow rate instrument were utilized to determine the

injection duration. The injected mass of ammonia and diesel for each test condition was determined using a Coriolis mass flow meter installed in-line with the respective fuel supply line. Coriolis meters provide direct mass flow rate measurement and are widely used because the measured variable is fundamentally proportional to mass flow (and not volumetric flow), thereby reducing sensitivity to density variations caused by pressure and temperature fluctuations. Liquid ammonia was injected at a fixed rail pressure of 200 bar and a controlled fuel temperature of approximately 300 K, ensuring subcooled liquid conditions at the injector inlet. Under these conditions, ammonia density variations prior to injection are negligible relative to in-cylinder thermodynamic changes. Accordingly, a constant inlet liquid density was specified for spray initialization, while subsequent density, phase change, and vaporization effects were resolved dynamically using the evaporation and breakup sub-models during spray evolution. **Equation (1)** demonstrates that the ammonia energy fraction represents the ratio of ammonia energy to the overall energy input of the fuel in the system.

$$\%AEF = \frac{\dot{m}_{NH_3} LHV_{NH_3}}{\dot{m}_{NH_3} LHV_{NH_3} + \dot{m}_{diesel} LHV_{diesel}} x100 \quad (1)$$

In **Equation (1)**, ṁ denotes the injected fuel mass per cycle, and LHV represents the lower heating value of each fuel. The ammonia energy fraction (AEF) is therefore defined on a per-cycle chemical energy basis, ensuring a constant total energy input across all test conditions, as commonly adopted in dual-fuel combustion studies **[11]**.

The equivalence ratio of the ammonia-diesel (AD) mixture can be determined utilizing **Equation (2)**.

$$\phi = \frac{\dot{m}_{diesel} / AFR_{St,diesel} + \dot{m}_{NH3} AFR_{St,NH3}}{\dot{m}_{Air}} \quad (2)$$

Here, ṁair stands for the mass of air inside the cylinder, while AFR stands for the air-fuel ratio.

Table 3: Experimental condition.

Parameter	Ammonia	Diesel
Injection system pressure (bar)	200	500
Start of injection range (°BTDC)	0°–40°	10°
Ammonia energy fraction (%)	10–90%	0–90%
Starting pressure	1 atm	
CR	19	
Initial charge temperature	353 K	
Test engine (crankshaft) speed	240 rpm	

The CONVERGE CFD 3.0 program was utilized to conduct the simulation modelling analyses. The complete shape of the combustion chamber was utilized for closed-cycle simulations. A turbulence model is essential for obtaining precise results from CFD simulations, as turbulence profoundly influences the rates of energy, momentum, and species mixing. When simulating anisotropic and non-equilibrium effects, the RNG k-ε model of turbulence **[12]** produce a better accuracy than on the conventional k-turbulence model. The discretized Navier-Stokes equations on a Cartesian grid were solved using an indirect finite volume discretization technique. The computer accelerates the process by simulating the three phases of expansion, compression, and combustion, using experimental data to determine the starting fuel, air conditions, and temperature of the environment. Until the experimental driving pressure is reached, the original temperature, flow velocity, and pressure are maintained.

Table 4: CONVERGE Sub-Models Applied in This Work

Physical process	Physical process
Turbulence behavior	RNG k- ε formulation **[12]**
Droplet aerodynamic resistance	Dynamic drag treatment **[13]**
Droplet breakup mechanism	KH-RT fragmentation model**[14]**
Inter-droplet collision	NTC collision model**[15]**
Evaporation of liquid droplets	Frossling-based evaporation model **[16]**
Turbulent dispersion of droplets	TKE preserving dispersion model**[13]**
Chemical kinetics solver	SAGE combustion solver **[17]**

The SAGE detailed chemistry solver was coupled with an ammonia oxidation mechanism, including nitrogen sub-chemistry relevant to NO formation. The mechanism selection follows recent ammonia combustion studies emphasizing NOx sensitivity to kinetic pathways **[18]**.

N-heptane (C7H16) was used to model diesel fuel. N-heptane straight-chain (C7H16) is a good replacement for diesel since it has similar ignition delay and heat release rate (HRR) in engines. Diesel and ammonia (NH3) were added to the system using Lagrangian particles. The size of the aperture affected how the droplets spread out. Liquid-phase ammonia and diesel sprays were modeled using the Kelvin–Helmholtz Rayleigh–Taylor (KH–RT) breakup model. The KH mechanism governs primary

jet surface instabilities near the nozzle exit, while the RT mechanism describes secondary breakup driven by aerodynamic acceleration. This combined KH–RT framework is widely adopted for high-pressure fuel injection in engine-relevant conditions **[14]**. Although ammonia exhibits different thermophysical properties compared to diesel, such as lower surface tension, lower viscosity, and high latent heat of vaporization, the KH–RT model remains applicable for representing liquid jet destabilization under high-pressure injection, provided that fuel-specific properties are correctly specified **[19]**. The SAGE chemical solver was used to find out how fast the combustion happened **[43]**. Before executing the transport calculation, it is essential to ascertain the reaction rates for the fundamental processes at each time step and the mass fractions of the new species. A source is defined as a condition in which the bulk fractions of the species undergo alteration. The system and the transport solver are connected via the species transport equation's source term. To expedite the computer modeling, the chemical and flow solvers operate concurrently. All combustion chamber walls, including the piston crown, cylinder liner, and cylinder head, were treated as isothermal boundaries with a prescribed wall temperature. The wall temperature was set to a constant value representative of a thermally stabilized engine operating condition and was kept identical for all simulation cases to ensure that observed differences in ignition delay, peak temperature, and emissions arise solely from fuel composition and injection timing effects. Convective heat transfer between the in-cylinder gases and the combustion chamber walls was modeled using the standard wall heat transfer formulation implemented in CONVERGE. Radiative heat transfer was neglected due to its relatively minor contribution under the investigated operating conditions. The same heat transfer model and boundary conditions were applied consistently across all cases to enable a fair comparison of combustion and emission trends.

2. Result and Discussion

3.1. Validation

The simulation modeling in-cylinder pressure of Ammonia energy fraction (AEF) 0%, 20%, and 40% was validated using experimental data. **Figure 2** compares in-cylinder pressure to the fluctuation of ammonia energy fraction. No substantial discrepancies existed between the experimental and simulation validation data. In each case, the smallest variance is below 5%, and the experimental and simulation pressures are closely aligned.

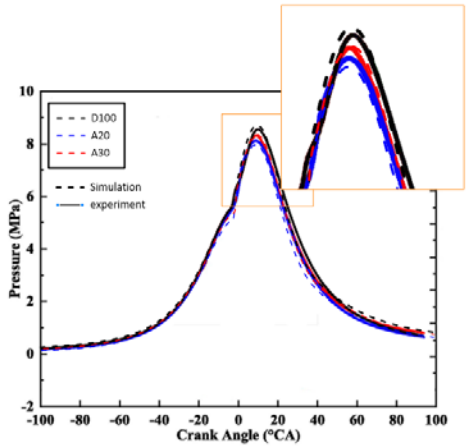

Figure 2: The comparison between simulation and experimental data of the pressure in the ammonia-diesel dual fuel engine **[20]**.

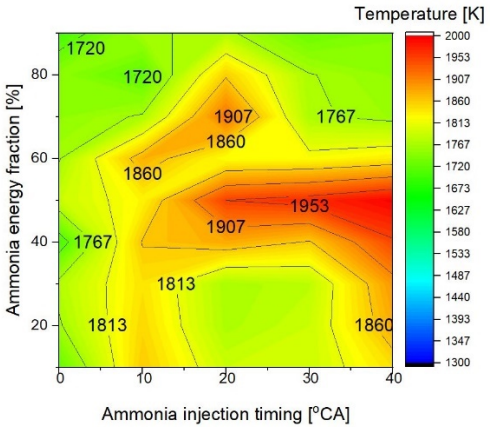

Figure 3. Maximum in-cylinder temperature of an ammonia engine as influenced by variations in ammonia energy fraction and start of injection (SOI) of ammonia.

The modeling results will be employed to examine the intricate emission dispersion of dual-fuel ammonia-DI engines.

3.2. Maximum Temperature

The evolution of maximum in-cylinder temperatures with respect to AEF and changes in ammonia injection timing is depicted in **Figure 3**. The maximum in-cylinder temperature reported in this study refers to the instantaneous local peak temperature obtained from CFD simulations. The injection of liquid-phase ammonia induces charge cooling through latent heat absorption and enhanced wall heat transfer, which can suppress local reaction rates at high ammonia fractions. Ammonia fuel did not completely burn at the first stage of combustion. Ammonia's low temperature lowers the surrounding air temperature. Additionally, injecting ammonia into the liquid phase prevents heat transfer. Increasing the ammonia percentage and injecting

ammonia before 20 degrees before top dead center (°BTDC) allowed for a constant increase in the peak in-cylinder temperature at a 50% ammonia energy fraction. In comparison to 0°BTDC and 20°BTDC SOIs of ammonia, a 10°BTDC SOI yields a little higher temperature. This results from the unchanged deterioration of ambient temperature induced by premature ammonia injection. Consequently, diesel's auto-ignition capabilities are improved. The peak in-cylinder temperature decreases when the ammonia energy component rises above 50%. In these circumstances, an earlier ammonia injection timing results in a smaller increase in the in-cylinder temperature.

3.3 Indicated Thermal Efficiency

The indicated thermal efficiency (ITE) of the engine at a compression ratio of 19 is depicted in **Figure 4**, where ammonia concentration varies from 10% to 90% and injection timing ranges from 0° to 40° BTDC. The indicated thermal efficiency (ITE) was evaluated based on the ratio of indicated work obtained from pressure–volume integration to the total chemical energy input per cycle, consistent with RCEM-based efficiency analysis methodologies. When ammonia was initially introduced, the ITE with less than 50% ammonia demonstrated improvement. Reducing ammonia application while maintaining a constant fuel injection pressure decreases ambient temperature and diminishes the likelihood of larger fuel discharge droplets. In this instance, an enhanced air-fuel mixture and superior combustion quality are achieved through earlier injection timing in conjunction with a prolonged ignition delay. Ammonia and diesel were concurrently injected at 10 degrees before top dead center (BTDC) in order to attain the minimum indicated thermal efficiency (ITE) in lean ammonia mixtures. Following the addition of ammonia subsequent to the diesel injection timing (0° BTDC), the ITE exhibited

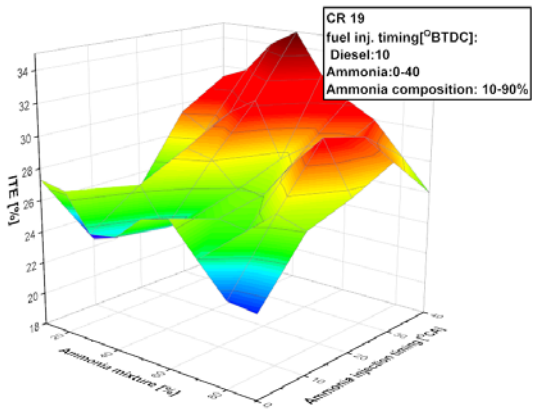

Figure 4: Indicated thermal efficiency of ammonia engine under variation of ammonia energy fraction and SOI of ammonia

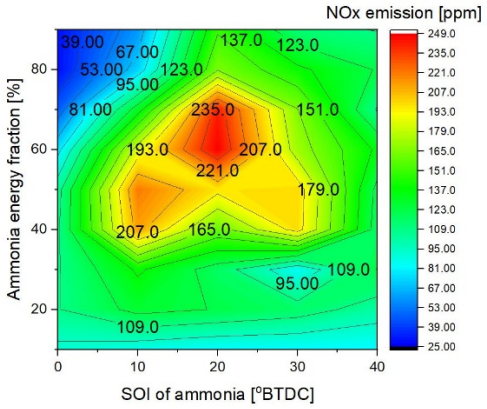

Figure 5: Total NO_x emission under variation of ammonia energy fraction and SOI of ammonia

improvement. A reduced ITE was observed due to an early administration timing involving more than 50% ammonia. The ambient temperature and pressure must increase in proportion to the rise in ammonia content due to its high-octane characteristics. The phase of liquid of ammonia reduces the temperature inside the cylinder and impedes the auto ignition mechanism of diesel under non-reactive conditions. An increased quantity of ammonia elevates the likelihood of in-cylinder wall wetting when ammonia is injected early, which reduces the wall temperature of the cylinder and results in bigger fuel droplets adjacent to the wall. The timing of ammonia injection between 20° and 30° BTDC enhanced the ITE. The indicated thermal efficiency markedly declined when ammonia was injected nearer to the top dead center.

3.4 The Emission of Nitrogen Oxides (NO_x)

With an ammonia SOI of 10° to 30° BTDC, the increased concentration of NOx was clearly generated at ammonia concentrations ranging from 40% to 80%. Thermal NOx is made when oxygen and nitrogen in the air of a fire react with each other at high temperatures. The main source of NOx emissions during the burning of gasses and light oils is thermal NOx. The rate of NOx generation usually increases noticeably at temperatures higher than 1773 K **[21]**. Thermal NOx formation is primarily associated with the oxidation of atmospheric nitrogen (N_2) at high temperatures, while ammonia additionally introduces fuel-bound nitrogen, contributing to NO formation through distinct reaction pathways **[21]**. The area experiencing the maximum temperature exhibited the greatest concentration of NOx. However, compared to 20 and 30 degrees before top dead center (BTDC) SOI of ammonia, 40 degrees BTDC SOI of ammonia yields the highest peak in-cylinder temperature and a reduced NOx concentration.

This signifies that specific areas of the fuel fail to ignite because of the wall-wetting effect, and that the premature introduction of ammonia leads to a swift reduction in flame propagation during the second phase of ammonia combustion, attributed to the improved quality of the air-fuel combination. The reduction in flame surface area, which is essential for NOx formation, accounts for the low NOx emissions observed during the initial phase of ammonia injection. Even with the assistance of diesel's auto-ignition, ammonia's auto-ignition took place significantly later, despite being administered prior to diesel. It demonstrated that reduced temperatures and pressures during combustion resulted from certain portions of ammonia contacting the cylinder wall.

The initial charge composition inside the RCEM cylinder was defined as fresh dry air, consisting of 21 vol.% O_2 and 79 vol.% N_2. The initial in-cylinder pressure and temperature were set according to the experimental conditions listed in **Table 3**. This controlled composition ensures repeatable ignition and combustion behavior across all test cases. Due to the single-cycle operation of the rapid compression expansion machine, residual exhaust gases from previous cycles were neglected. As a result, the residual gas fraction was assumed to be zero for all experimental and numerical cases, eliminating dilution effects associated with internal exhaust gas recirculation. Although the maximum in-cylinder temperature increased at an ammonia start of injection (SOI) of 40° BTDC, the corresponding NOx emissions were reduced compared to intermediate injection timings. This behavior indicates that NOx formation cannot be interpreted solely based on peak temperature values. Thermal NOx formation is strongly influenced by the residence time of gases at elevated temperatures, the volume fraction of regions exceeding the critical NOx formation temperature, and the local availability of oxygen under near-stoichiometric conditions. At advanced ammonia injection timing, early fuel introduction enhances premixing and mixture dilution, which reduces the spatial extent of stoichiometric high-temperature zones despite the presence of localized temperature peaks. Furthermore, early liquid-phase ammonia injection intensifies wall heat absorption and charge cooling near the cylinder boundaries, leading to shorter residence times at temperatures favorable for NOx formation. As a result, even though localized peak temperatures may increase, the overall integrated NOx production is reduced due to diminished high-temperature reaction zones and limited oxygen availability in fuel-rich or highly diluted regions.

In this study, nitrogen oxide (NOx) emissions were evaluated as the primary nitrogen-containing exhaust species. Due to experimental constraints associated with the RCEM configuration, unburned ammonia (NH_3 slip) and nitrous oxide (N_2O) emissions were not directly measured. These species are recognized as important nitrogen-fate pathways in ammonia-fueled engines and should be addressed in future studies using dedicated exhaust analysis systems **[20]**. Therefore, the present results focus on relative NOx trends and combustion behavior rather than a complete nitrogen balance. It should be noted that nitrogen oxide (NOx) emissions were evaluated as the primary nitrogen-containing exhaust species in this study. Due to experimental constraints associated with the rapid compression expansion machine (RCEM) configuration, unburned ammonia (NH_3 slip) and nitrous oxide (N_2O) emissions were not directly measured. These species are known to play a critical role in ammonia-fueled combustion systems, where reductions in NOx may be accompanied by increased NH_3 slip or N_2O formation depending on injection strategy and combustion temperature.

3.5 CO/CO_2 Formation

Figure 6 illustrates the in-cylinder distributions of temperature, CO, and CO_2 emissions of a diesel flame at various crank angles (0°, 10°, 20°, 30°, and 40°), highlighting the combustion and oxidation progression within the chamber. At the early stage (0°–10°), the temperature is relatively low (800–1300 K), and the combustion is still developing. As the crank angle advances to 20°, a high-temperature region above 1700 K forms at the core, marking the onset of intense combustion and CO formation. The CO distribution shows that its maximum concentration occurs around 1700 K, indicating incomplete combustion under locally fuel-rich conditions. As the temperature continues to rise beyond

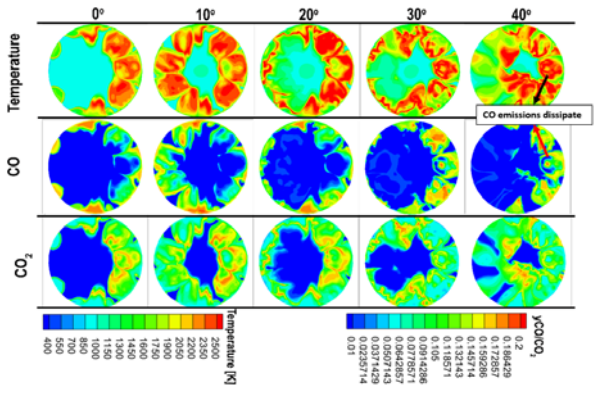

Figure 6: Correlation of CO/CO_2 formation against in-cylinder temperature

2000 K, CO gradually oxidizes to CO_2, and by 30°–40°, CO emissions nearly disappear, demonstrating complete oxidation. The CO_2 concentration, initially low in early stages, increases significantly as the temperature rises and combustion proceeds, reaching its peak at 2000 K and above, corresponding to complete oxidation zones. These results confirm that CO formation peaks at the 1700 K zone and ceases once the temperature exceeds 2000 K, while CO_2 generation increases concurrently, illustrating the strong dependence of emission behavior on combustion temperature and indicating efficient oxidation and combustion completion in high-temperature regions.

4. Conclusion

This study comprehensively investigated the combustion and emission characteristics of an ammonia–diesel dual direct injection compression ignition (CI) engine through combined experimental and numerical approaches using a rapid compression expansion machine (RCEM) and CFD simulation. The results demonstrated that the ammonia energy fraction (AEF) and the start of injection (SOI) timing of ammonia significantly influence in-cylinder temperature, ignition delay, and emission formation. Early ammonia injection (before 20° BTDC) improved the air–fuel mixing process and increased the indicated thermal efficiency (ITE) when the AEF was below 50%. However, at higher AEF values (>50%), excessive ammonia substitution and early injection led to a decrease in peak temperature due to the cooling effect of liquid-phase ammonia and wall-wetting phenomena, resulting in incomplete combustion and reduced efficiency. The formation of NOx was strongly correlated with regions of high temperature (>1773 K), while excessive early injection reduced NOx due to limited flame propagation and smaller high-temperature zones. The CO and CO_2 distributions revealed that CO formation peaked around 1700 K and was almost completely oxidized into CO_2 as the in-cylinder temperature exceeded 2000 K, confirming that higher combustion temperatures promote complete oxidation and lower incomplete combustion emissions. Although NOx trends were successfully analyzed, NH_3 slip and N_2O emissions were not quantified in the present study. These species represent critical environmental considerations for ammonia-fueled engines and will be addressed in future experimental campaigns. Overall, the findings highlight that optimal ammonia utilization in dual-fuel CI engines can be achieved by carefully balancing injection timing and substitution ratio to enhance combustion stability, thermal efficiency, and emission reduction. This research provides a foundation for optimizing ammonia-based combustion strategies toward achieving low-carbon and efficient alternative fuel engines.

Acknowledgement

- This work was supported by the National Research Foundation Korea(NRF) grant funded by the Korea government(MSIT) (No. RS-2023-00281590)
- This result was supported by the "Regional Innovation System & Education (RISE)" through the Ulsan RISE Center, funded by the Ministry of Education (MOE) and the Ulsan Metropolitan City, Republic of Korea.(2025-RISE-07-001)

Author Contributions

Conceptualization, A. Setiawan and O. Lim; Methodology, A. Setiawan; Software, A. Setiawan; Validation, A. Setiawan and O. Lim; Formal Analysis, A. Setiawan; Investigation, A. Setiawan; Resources, O. Lim; Data Curation, A. Setiawan; Writing—Original Draft Preparation, A. Setiawan; Writing—Review & Editing, O. Lim; Visualization, A. Setiawan; Supervision, O. Lim; Project Administration, O. Lim; Funding Acquisition, O. Lim.

References

[1] P. Price, S. Guo, and M. Hirschmann, “Performance of an evaporator for a LPG powered vehicle,” Applied Thermal Engineering, vol. 24, no. 8–9, pp. 1179–1194, 2004.

[2] D. G. Snelgrove, P. Dupont, and R. Bonetto, “An investigation into the influence of LPG (autogas) composition on the exhaust emissions and fuel consumption of 3 bi-fuelled renault vehicles,” SAE Technical Paper, 1996.

[3] J. Sun, N. Zhao, and H. Zheng, “A comprehensive review of ammonia combustion: Fundamental characteristics, chemical kinetics, and applications in energy systems,” Fuel, vol. 394, p. 135135, 2025, doi: https://doi.org/10.1016/j.fuel.2025.135135.

[4] K. Kim, J. Kim, S. Oh, C. Kim, and Y. Lee, “Lower particulate matter emissions with a stoichiometric LPG direct injection engine,” Fuel, vol. 187, pp. 197–210, 2017.

[5] S. Baek, K. Kim, J. Cho, C.-L. Myung, and S. Park, “Assessment of gaseous, particulate, and unregulated emissions from diesel compression ignition and LPG direct injection spark ignition minibus vehicles under the world harmonized vehicle cycle on a chassis dynamometer,” Fuel, vol. 294, 120392, 2021.

[6] C. Windarto and O. Lim, “A comprehensive study of the effects of spark discharge duration on low-carbon combustion of high-pressure direct-injection propane: Factors affecting combustion, in-cylinder performance, and emissions,” International Journal of Hydrogen Energy, vol. 49, pp. 796–815, 2024.

[7] H. Ambarita, “Performance and emission characteristics of a small diesel engine run in dual-fuel (diesel-biogas) mode,” Case Studies in Thermal Engineering, vol. 10, pp. 179–191, 2017.

[8] S. Ouchikh, M. S. Lounici, L. Tarabet, K. Loubar, and M. Tazerout, “Effect of natural gas enrichment with hydrogen on combustion characteristics of a dual fuel diesel engine,” International Journal of Hydrogen Energy, vol. 44, no. 26, pp. 13974-13987, 2019.

[9] F. Oliva and D. Fernández-Rodríguez, “Autoignition study of LPG blends with diesel and HVO in a constant-volume combustion chamber,” Fuel, vol. 267, p. 117173, 2020.

[10] A. Fakhari, A. Gharehghani, M. Salahi, A. M. Andwari, et al., “Numerical investigation of ammonia-diesel fuelled engine operated in RCCI mode,” SAE Technical Paper 2023-24-0057, 2023.

[11] M. Lang, Y. Su, Y. Wang, Y. Zhang, B. Wang, and S. Chen, “Experimental study on the effects of pilot injection strategy on combustion and emission characteristics of ammonia/diesel dual fuel engine under low load,” Energy, vol. 303, 131913, 2024

[12] Z. Han and R. D. Reitz, “Turbulence modeling of internal combustion engines using RNG κ-ε models,” Combustion Science Technology, vol. 106, no. 4-6, pp. 267-295, 1995.

[13] B. S. de Lima, K. C. Fagundes, G. R. C. Faria, M. H. B. Sandoval, and C. E. C. Alvarez, “Encit2018-0458 Analysis of the combustion process in an engine adapted with pre-chamber using a zero dimensional numerical model and a three-dimensional model,” 17th Brazilian Congress of Thermal Sciences and Engineering, November 25th-28th, 2018, Águas de Lindóia, SP, Brazil, 2018.

[14] R. D. Reitz, “Mechanism of breakup of round liquid jets,” Encyclopedia of Fluid Mechanics, vol. 10, 1986.

[15] D. P. Schmidt and C. J. Rutland, “A new droplet collision algorithm,” Journal of Computational Physics, vol. 164, no. 1, pp. 62–80, 2000.

[16] A. A. Amsden, P. J. O’Rourke, and T. D. Butler, “KIVA-II: A computer program for chemically reactive flows with sprays,” Los Alamos National Lab.(LANL), Los Alamos, NM (United States), 1989.

[17] C. Windarto and O. Lim, “Spark discharge energy effect on in-cylinder characteristics performance of rapid compression and expansion machine with spark ignition direct injection strategy,” Fuel, vol. 337, 127165, 2023.

[18] K. D. K. A. Somarathne, et al., “Emission characteristics of turbulent non-premixed ammonia/air and methane/air swirl flames through a rich-lean combustor under various wall thermal boundary conditions at high pressure,” Combustion and Flame, vol. 210, pp. 247-261, 2019.

[19] A. Valera-Medina, et al., “Review on ammonia as a potential fuel: from synthesis to economics,” Energy & Fuels, vol. 35, no. 9, pp. 6964–7029, 2021.

[20] Q. Zuo, et al., “Performance analysis of ammonia energy ratio on an ammonia-diesel engine in different fuel supply modes,” Fuel, vol. 384, 134038, 2025, doi: https://doi.org/10.1016/j.fuel.2024.134038.

[21] S. Wu, D. Che, Z. Wang, and X. Su, “NOx emissions and nitrogen fate at high temperatures in staged combustion,” Energies, vol. 13, no. 14, 2020, doi: 10.3390/en13143557.